

## II. DEVICE DESCRIPTION AND GENERAL PHYSICS REQUIREMENTS

G. H. NEILSON, Jr. (ORNL)

### II.A. INTRODUCTION

To accomplish the dual goals set forth in the mission statement — determination of burning plasma physics and demonstration of fusion power production — requires a tokamak with special characteristics. A conceptual design for such a facility has been developed by the CIT/BPX Project team over a period of about 5 years. The process has drawn extensively upon the world tokamak physics data base as well as engineering experience gained on actual machines like Tokamak Fusion Test Reactor (TFTR) and the Alcators and on design studies for machines like the Long-Pulse Ignited Test Experiment (LITE) and the Tokamak Fusion Core Experiment (TFCX). The Joint European Torus (JET) and Doublet III-D (DIII-D) experiments in particular have had a significant influence on the physics base. The resulting design incorporates features that have proven successful in tokamak experiments, combined with new features that are needed in the regime of high-power-density deuterium-tritium (D-T) fusion plasmas.

The design of the BPX device and facility is based on a set of requirements developed from both physics and engineering considerations. Collectively, the requirements define the necessary hardware capabilities for a tokamak facility to accomplish the BPX mission. They are contained in the Project's General Requirements Document (GRD) and System Requirements Document (SRD). The former specifies general machine characteristics such as major parameters, heating, energy handling, and diagnostic capabilities. The latter specifies requirements for individual BPX subsystems at a more detailed level. The requirements have been carefully developed to be consistent with both engineering and physics criteria. From the engineering perspective, each requirement must have a conceptual design solution that satisfies engineering criteria and is included in the overall cost estimate. From the physics side, the requirements must be supported by data and analysis that show that a facility that meets these requirements will accomplish the BPX mission.

In many aspects, tokamak physics models have reached a high degree of sophistication and accuracy. In other aspects, however, there is considerable uncertainty, making it impossible to make

precise projections. For example, the estimated uncertainty in projecting energy confinement time for BPX is about  $\pm 25\%$ , not including uncertainties in  $Z_{eff}$  and profiles, nor possible alpha-particle effects. To incorporate enough margin to guarantee the high-end BPX performance goals (near-ignition with  $P_{fus} = 500$  MW) in the face of such uncertainties would result in an extremely large and prohibitively expensive machine. Clearly, to preclude such performance would unnecessarily restrict BPX's research potential. On the other hand, to achieve less than the minimum goals ( $Q = 5$  and  $P_{fus} = 100$  MW) would prevent BPX from meeting its burning plasma physics objectives and would constitute too small a step in fusion energy development. Recognizing these facts, the BPX mission specifies a range of goals. To translate the mission statement into appropriate design requirements, the following physics design philosophy has been followed:

1. **Performance.** The plasma performance of BPX is determined by its major device parameters and its plasma control, heating, fueling, energy and particle handling, and disruption handling capabilities. The "minimum performance" level ( $Q = 5$ ,  $P_{fus} = 100$  MW) must be achieved with high confidence. By "high confidence," we mean that performance is projected using conservative physics assumptions. The device and facility must also be consistent with achieving the "standard performance" level ( $Q \approx 25$ ,  $P_{fus} = 500$  MW) that would be expected on the basis of standard physics assumptions that we have carefully developed. This distinction mainly arises in those areas where accurate physics projections are not possible, such as confinement and power handling. In tokamak experiments, "standard" performance in this sense is only obtained after significant optimization in the operations phase. To ensure that BPX will have the means to optimize performance, flexibility becomes an explicit requirement.
2. **Flexibility.** The device must incorporate the flexibility needed to optimize operation and to accomplish the broad range of research objectives specified in the mission statement. Examples of flexibility include a variety of mag-

netic configurations, several wall conditioning options, and provision for multiple heating and fueling systems. The capability to replace or modify internal device hardware and peripheral equipment, even after the facility has become activated, is also necessary in order to allow for the incorporation of new developments.

3. **Diagnostics.** The facility must incorporate the diagnostics needed to characterize the plasma behavior and provide operational data. A range of alpha-particle measurements is clearly required. The main plasma parameters must be accurately determined as functions of space and time in order to explain the physical mechanisms that determine overall behavior. Other diagnostics are needed for operational purposes.

This design philosophy will be elaborated in much more detail in subsequent chapters. The physics data, models, analysis, and criteria that support the requirements and specific design solutions will be described. By way of introduction, those general requirements that have a physics basis are reviewed in the remainder of this chapter, along with the main features of the BPX tokamak design. However, detailed engineering descriptions are outside the scope of this paper.

## II.B. MAJOR DEVICE PARAMETERS

The BPX must achieve fusion plasma performance levels much higher than any obtained or projected for existing machines. Under standard performance conditions, the ignition parameter  $\langle n_e T \rangle \tau_E$  will be over  $2.5 \times 10^{21} \text{ m}^{-3} \cdot \text{keV} \cdot \text{s}$ . To achieve such performance, the BPX uses a high magnetic field ( $B_T = 9 \text{ T}$ ) approach, in the tradition of the Alcator-A, Alcator-C, and the proposed LITE devices. A high-elongation, poloidal divertor configuration similar to those of DIII-D and JET is used to provide the high plasma current and H-mode conditions needed for good confinement. Heating in the ion cyclotron range of frequencies (ICRF) is used, as in TFTR and JET, to raise the temperature. An elevation view of the device is shown in Fig. 2.1, and major parameters, as specified in the GRD, are summarized in Table 2.1.

The machine parameters have been chosen to provide the required level of projected plasma performance and to operate in the relevant burning plasma physics regime to carry out the BPX mission. Alpha-particle issues, stability limits, and energy handling are among the more important physics considerations affecting these choices. Since the major parameters are especially tied to

projections of plasma energy confinement, this subject has been studied in a number of ways, and the reader is referred to Chap. III for a more complete discussion of the various approaches. However, the physics basis for the selected set of major parameters may be understood at a simple level by considering projections based on empirical global scaling and prescribed profiles. A "standard" performance model is used based on extensive analysis of the world tokamak data base. Characteristics of this model are summarized in Table 2.2.

We base our standard confinement projections on the L-mode power law scaling developed by the ITER Physics Team,<sup>1</sup> multiplied by an H-mode enhancement factor ( $c_\tau$ ) of 1.85:

$$\begin{aligned} \tau_E &= 1.85 \times \tau_L^{ITER-89P} \\ &= 1.85 \times 0.0381 A_i^{0.5} I_p^{0.85} B_T^{0.2} \bar{n}_{e19}^{0.1} \\ &\quad R_0^{1.2} a^{0.3} \kappa^{0.5} P_{heat}^{-0.5} \text{ s} \end{aligned}$$

with  $A_i$  in amu,  $I_p$  in MA,  $B_T$  in T,  $\bar{n}_{e19}$  in  $10^{19} \text{ m}^{-3}$ ,  $R_0$  and  $a$  in meters, and  $P_{heat}$  in MW. An important objective for BPX is to determine whether the alpha-particle heating efficiency will be degraded by alpha losses or alpha-induced effects on bulk confinement; however, our projections effectively assume that the heating efficiency is equivalent to that of the existing auxiliary heating data base. With this model, the BPX parameters provide an operating space that is represented by a plot of Plasma Operation CONtours (POP-CONs) in Fig. 2.2. The region bounded by the  $Q = 5$  contour, the  $P_{fus} = 500 \text{ MW}$  contour, and the  $P_{aux} = 20 \text{ MW}$  contours constitutes a wide regime in which to study burning plasma physics effects. By way of example, an approximate stability boundary for the alpha-driven toroidal Alfvén eigenmode (TAE) divides this region, as shown in the POPCON diagram. The ability of BPX to operate on either side of the boundary will facilitate the study of the TAE and its effects on the plasma. The standard operating region lies well within more established stability boundaries such as the Troyon beta limit and the Greenwald density limit. Furthermore, with  $\kappa_{95} \approx 2$  and  $q_{95} \geq 3.2$ , BPX is in a regime where vertical stability and disruption-free operation are obtainable. As with confinement, to determine how operating limits might be modified in burning plasmas is an objective of the experiment. Projections are based on the well-established operating limits derived from the present data base, however.

Heating power upgrades to 50 MW could further expand the operating region and increase flexibility. However, the minimum auxiliary heating power requirement is determined by time-

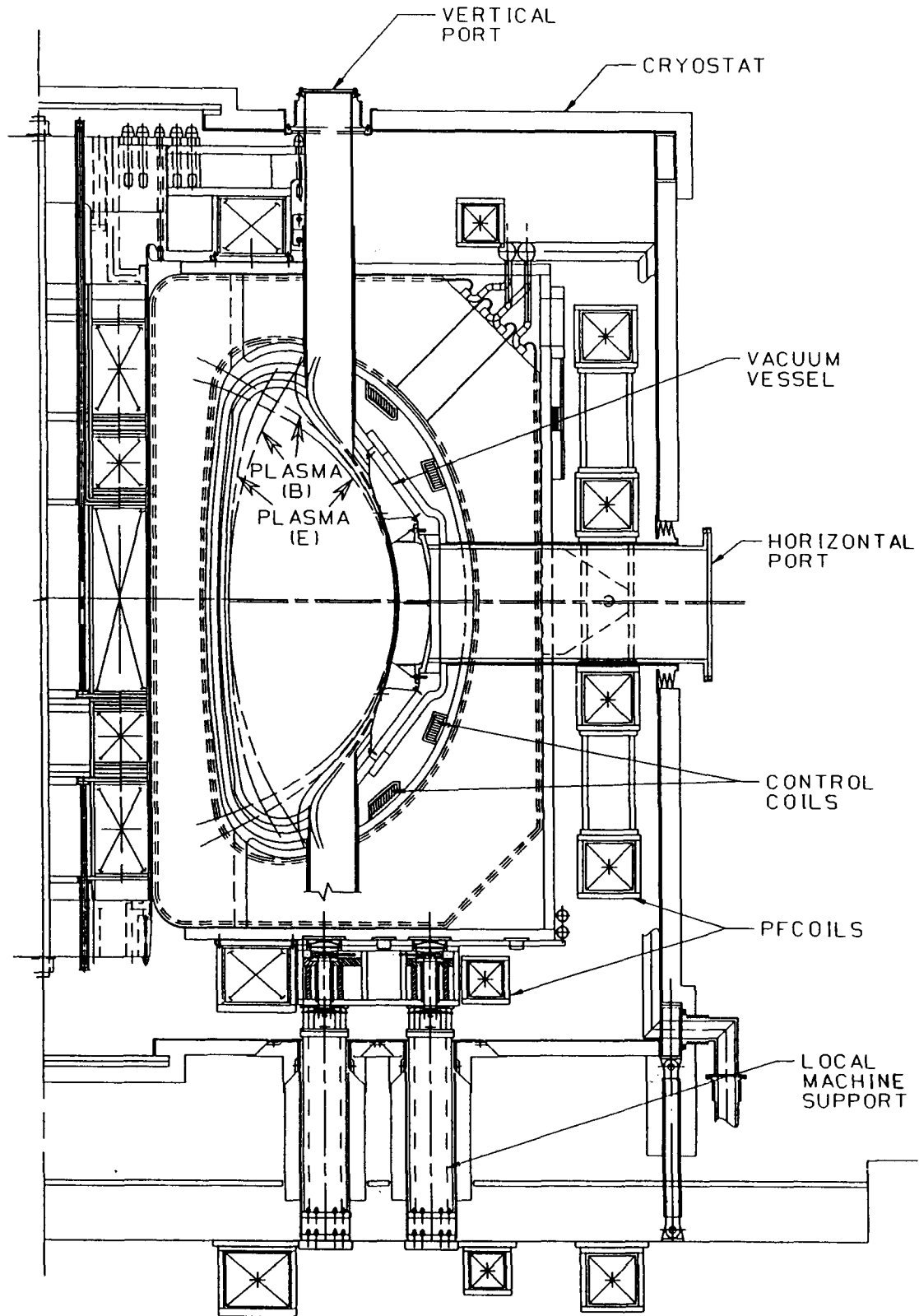


Fig. 2.1. Elevation view of the BPX device. Two plasma boundaries are shown, corresponding to the beginning of flattop (B) and end of burn (E) in the DN divertor reference operating mode.

Table 2.1. BPX Device Parameters

( ) = upgrade capability

Major radius, $R_0$	2.59	m
Minor radius, $a$	0.80	m
Toroidal magnetic field, $B_T$	9.0	T
Plasma current, $I_p$	11.8	MA
Elongation, $\kappa_{95}$	2	
Triangularity, $\delta_{95}$	0.25 – 0.45	
Safety factor, $q_{95}$	$\geq 3.2$	
$B_T/I_p$ flattop time, $t_{flat}$	10	s
Fusion power, $P_{fus}$	100 – 500	MW
Plasma heating power:		
Alpha-particle, $P_\alpha$	20 – 100	MW
ICRF, $P_{ICRF}$	20 (30)	MW
Total $P_{aux}$ (ICRF + ECH)	20 (50)	MW
Number of pulses:		
At maximum $B_T$ and $I_p$	3,000	
At 2/3 maximum $B_T$ and $I_p$	30,000	
Pulse interval at maximum $B_T$ and $I_p$	60	min

Table 2.2. "Standard" BPX Performance Model

Energy confinement time	$1.85 \times \tau_L^{ITER-89P}$
Density profile shape	$[1 - (r/a)^2]^{\alpha_n}$ ; $\alpha_n = 0.5$
Temperature profile shape	trapezoidal (break at $r/a = 1/q_{95}$ )
$Z_{eff}$	1.65 (carbon and 3% helium)

dependent considerations. Enough power must be provided to heat the plasma to near-ignition conditions, leaving several seconds of flattop burn time for physics studies. We have adapted our zero-dimensional performance model (Table 2.2) to the time-dependent problem by replacing " $P_{heat}$ " with " $W/\tau_E$ " in the empirical scaling formula, since it is physically more reasonable to assume that confinement time is determined by stored energy ( $W$ ) than by heating power. The amount of power required is a sensitive function of the H-mode multiplier. With a multiplier of 2.0, the baseline complement of 20 MW will be sufficient to reach the limits of the device's energy handling capability ( $P_{loss} = 100$  MW, for a 3-s flattop), as shown in Fig. 2.3. Decreasing the H-mode multiplier from 2.0 to 1.85 decreases the flattop burn time because of energy handling limitations, unless the auxiliary heating power is increased from 20 to 26 MW. The BPX device and facility can accommodate an upgrade to 30 MW of ICRF power, or up to 50 MW of ICRF plus electron cyclotron heating (ECH) power, if necessary. Details of the time-dependent zero-dimensional calculations are presented in Sec. III.D.

With more pessimistic performance projections, the capability for burning plasma studies is correspondingly reduced. However, the standard model provides enough physics margin that the minimum performance requirement ( $P_{fus} = 100$  MW,  $Q = 5$ ) can still be met. Monte Carlo studies in which the model parameters are varied randomly over their ranges of uncertainty have been performed to assess the uncertainty in performance projections (Sec. III.D). Plasma parameters for typical operating points, corresponding to standard and minimum performance levels, are given in Table 2.3. The standard performance case is constrained to have  $P_{loss} = 100$  MW, corresponding to our standard model for divertor power handling capability. Up to 500 MW of fusion power can be achieved with standard confinement ( $c_\tau = 1.85$ ) and more optimistic divertor performance, or with slightly more optimistic confinement ( $c_\tau \approx 2$ ) and the standard divertor performance model. The minimum performance case is projected using values of H-mode enhancement factor, density profile exponent  $\alpha_n$  (defined in Table 2.2), and  $Z_{eff}$  on the pessimistic side of our standard model. This is a representative combination of parameters from

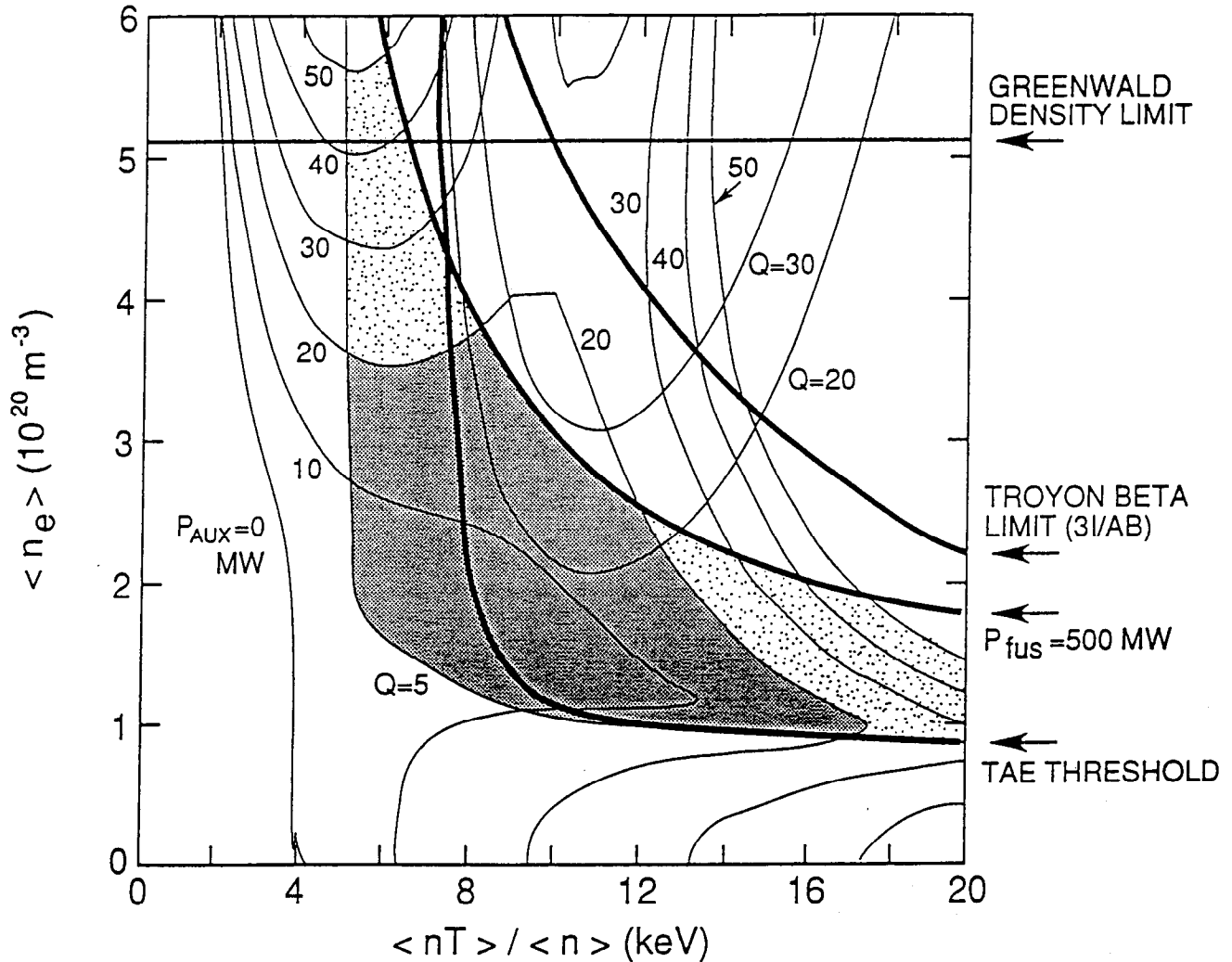


Fig. 2.2. Plasma operation contours for standard performance model. Dark shaded region indicates burning plasma operating space bounded by  $Q = 5$ ,  $P_{fus} = 500 \text{ MW}$ , and the baseline auxiliary heating complement of 20 MW. Light shaded region shows extended operating space with maximum upgrade heating power of 50 MW.

the Monte Carlo survey described above and in Sec. III.D. Time-dependent zero-dimensional calculations show that the baseline 20 MW of heating power is adequate to reach these minimum performance conditions.

The major parameters obviously must satisfy engineering design criteria as well as physics requirements. The BPX's high magnetic field strengths, for example, lead to high stresses in the toroidal field (TF) coils. With the high plasma currents and stored energies, disruptions will result in large stresses in the vacuum vessel, first-wall attachments, and poloidal field (PF) coils. The high fusion power leads to large thermal loads on the divertor and limiter and to nuclear heating of the

coils and vessel. The required pulse lengths translate into volt-second requirements and coil heating. Choosing a particular engineering design and then determining the predicted and allowable stresses for that design is a complicated procedure that will not be discussed in detail here. However, satisfying the engineering criteria for a component while providing a given level of performance is often a matter of sizing. The PPPL Systems Code, which integrates physics, engineering, and costing models, was used to size the machine. In determining the major radius, space envelopes are allocated to each component as needed to satisfy the engineering criteria. The minor radius, plasma current, and toroidal field are varied at constant aspect ratio,

Table 2.3. Typical Plasma Parameters

Parameter	Performance Level		
	Standard	Minimum	
H-mode enhancement factor	1.85	1.60	
$\alpha_n$	0.5	0.2	
$Z_{eff}$	1.65	1.9	
Helium concentration ( $n_{He}/n_e$ )	3.0	1.0	%
Density ( $n_e$ )	2.73	1.61	$\times 10^{20} \text{ m}^{-3}$
Temperature $\langle T \rangle$	9.99	9.00	keV
Beta	2.69	1.38	%
$P_{fus}$	417	100	MW
$P_\alpha$	83.4	20.1	MW
$P_{aux}$	14.3	17.2	MW
$P_{OH}$	2.3	2.7	MW
$Q(P_{fus}/P_{heat})$	25	5	
Energy confinement time $\tau_E$	0.89	1.13	s

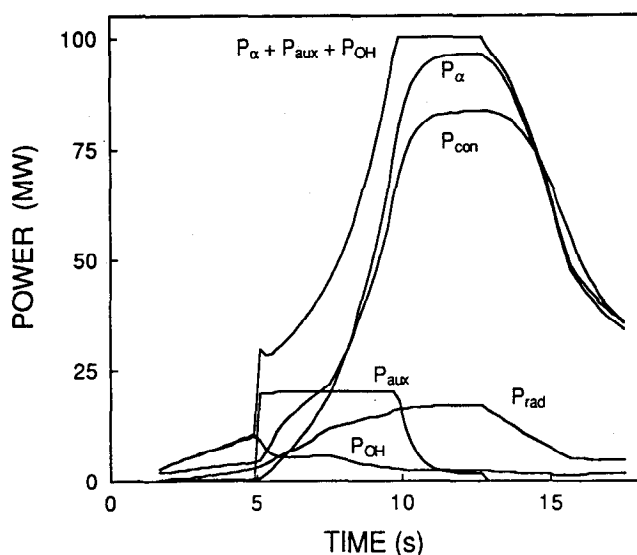


Fig. 2.3. Zero-dimensional, prescribed profile discharge simulation, showing plasma energy input from alpha-particle ( $P_\alpha$ ), auxiliary heating ( $P_{aux}$ ) up to 20 MW, ohmic heating ( $P_{OH}$ ), and total heating ( $P_\alpha + P_{aux} + P_{OH}$ ) power; and losses due to conduction ( $P_{con}$ ) and radiation ( $P_{rad}$ ). The standard BPX zero-dimensional performance model is used, except that the H-mode multiplier is 2.0.

safety factor, and ignition margin (based on a constant times ITER89-P scaling). For consistency, the code uses the same prescribed profile physics models (literally the same subroutine library) as are used in the POPCON (see Fig. 2.2) and other zero-dimensional physics analyses (Sec. III.D).

The choice of aspect ratio, 3.2, was confirmed by

a Systems Code scan at constant safety factor, ignition margin, and engineering margins. It is found that the BPX design point lies near a broad minimum in cost. It also lies near the middle of the range of aspect ratios covered by previous tokamaks, thereby ensuring a broad data base. Considerations of plasma shaping, heating frequency, and port access, which tend to favor low aspect ratio, were also factored in to the choice of aspect ratio.

In summary, the major device parameters chosen for BPX are consistent with its basic performance requirement: to achieve  $Q = 5$  and  $P_{fus} = 100$  MW with high confidence and to achieve near-ignition and  $P_{fus} = 500$  MW if confinement is sufficiently favorable. The former is projected using conservative physics assumptions, the latter using more typical ("standard") assumptions. The BPX parameters also provide a wide operating space in which to study burning plasma physics phenomena. The device's size parameters have been selected to ensure that both the physics requirements and the engineering constraints will be satisfied at minimum cost.

### II.C. REFERENCE OPERATING MODES AND ENERGY HANDLING

The BPX is designed to produce high peak fusion power and address physics issues that arise on energy confinement time scales. Equilibrium burn physics and long-pulse technology are beyond the scope of the BPX mission. This has allowed the use of such features as inductive current drive, liquid-nitrogen-cooled copper magnets,

passively cooled first-wall components, and minimal radiation shielding as a way of optimizing for high peak performance at minimum cost. On the other hand, time scales on the order of a few energy confinement times (i.e., a few seconds) at constant plasma parameters are required at a minimum to investigate (or confirm the absence of) possible effects such as a degradation of alpha heating efficiency. Therefore, certain measures are taken to maximize the useful pulse length obtainable with BPX's short-pulse technologies, for example:

### 1. Plasma initiation during $B_T$ rampup.

To make the most efficient use of the 10-s  $B_T$  flattop, plasma initiation, growth, current rampup, and initial heating are accomplished in the last 7.5 s of  $B_T$  rampup. An additional advantage of this strategy is that it is beneficial for MHD-stable current penetration. Since the total rampup time for  $B_T$  is  $> 20$  s,  $B_T$  is typically  $> 7.3$  T (5 T minimum) at the time of plasma initiation. By the time  $B_T$  reaches flattop, a fully elongated, full-current, high-temperature plasma is already established. After flattop, the toroidal field, plasma current, density, and cross section are reduced in a controlled manner so as to maintain stability.

### 2. Divertor sweeping.

Heat flux onto the divertor surface is concentrated in approximately a 6-cm-wide annulus adjacent to the separatrix. To maximize burn time without overheating the divertor (which would lead to impurity influx and possibly disruption), the separatrix is swept poloidally by about 20 cm, thereby distributing the heat loads over a wider area.

The dynamic performance requirements for BPX are specified in the GRD in terms of three "reference operating modes," a double-null divertor (DN), a single-null divertor (SN), and an inner-wall limiter (IW) mode. The device and facility must be capable of operating in any of these modes at full current, magnetic field, flattop pulse length, and auxiliary heating power. This requirement mainly drives the design of the PF, equilibrium control, heating, vacuum vessel, and energy handling systems. The requirements for the three reference modes define an operating envelope for BPX that affords considerable flexibility. A wide range of scenarios will be possible within this envelope, especially at less-than-maximum parameters.

In all three modes, the required  $B_T$  and  $I_p$  flattop pulse length is 10 s. The time-dependent plasma electromagnetic behavior is modeled using the Tokamak Simulation Code (TSC). Figure 2.4 illustrates the plasma growth from the outboard

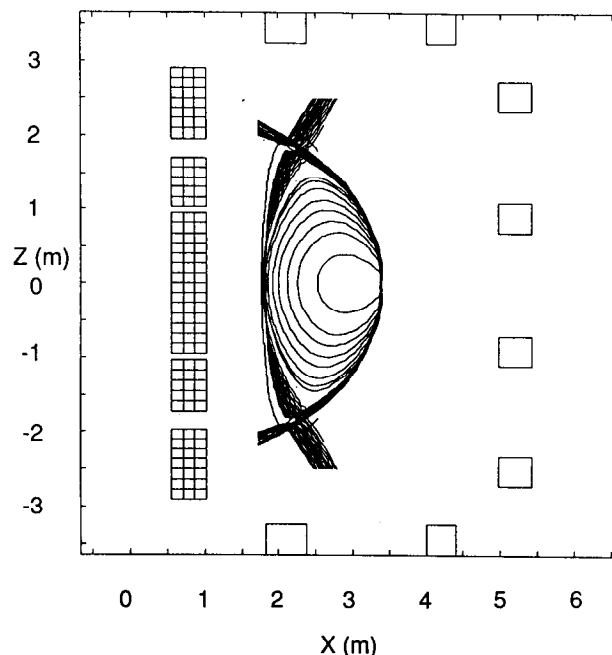


Fig. 2.4. Sequence of plasma boundaries during a reference DN divertor discharge, as calculated by Tokamak Simulation Code (TSC). Sequence shows plasma growth from the outboard limiter, divertor formation, and divertor sweeping.

limiters, as calculated using TSC. These studies, which are described more fully in Chap. V, help to determine the conditions needed to maintain stability and control during the plasma growth and shutdown phases. The important criteria are related to the current profile evolution and the avoidance of MHD stability limits in  $l_i$ - $q_{95}$  space. Other considerations that determine the  $B_T$  pulse shape are coil heating and power supply cost.

All operating modes must accommodate auxiliary heating during the rampup and rampdown as well the flattop phase. In particular, the plasma shape must conform well to that of the ICRF antenna over its entire length ( $\sim 1$  m) to ensure good radio-frequency (RF) coupling. Consequently, in all operating modes, the outboard plasma surface is required to conform within  $\pm 1$  cm to a reference surface parallel to the antenna and extending 0.48 m above and below the midplane. Certain requirements also apply to the heating systems themselves; for example, they must be capable of heating while the resonance is off-axis and must have pulse lengths of at least 15 s to overlap the rampup, flattop, and rampdown phases. Further details are provided in Chaps. VI (ICRF) and VII (ECH).

The three operating modes are mainly distinguished by their magnetic and energy handling configurations. The DN mode is depicted by the

two plasma outlines in Fig. 2.1, which correspond to the beginning of flattop (BOFT) and end of burn (EOB) times. The triangularity  $\delta_{95}$  is varied from 0.25 to 0.45 during the burn in order to sweep the separatrix as described earlier. Each X-point is required to stay at least 15 cm from its outboard and at least 10 cm from its inboard divertor target throughout the sweep. This requirement is the result of a trade-off between energy handling and impurity control considerations. While a closer spacing would lower the peak heat flux by increasing the expansion of the magnetic surfaces, it would also be expected to increase erosion by raising the plasma temperatures at the target surface. This issue is discussed further in Chap. IX. The capability exists to vary the spacings operationally either by changing the elongation in the DN configuration or by shifting the axis in the the SN configuration. These are important aspects of BPX's optimization flexibility. The GRD also requires a scrape-off channel between the separatrix and the open magnetic surface that intersects the outboard mid-plane 2 cm outside the separatrix. This so-called "2-cm surface" intersects no material components other than the divertor targets, thereby clearing the outer limiters and ICRF antennas. This requirement ensures a well-defined divertor configuration for establishing the H mode and providing unobstructed energy flow to the targets.

In the SN mode, the defining separatrix is swept across either the upper or lower divertor target only. The sweep and X-point-to-target spacing specifications are the same as for the DN mode. The 2-cm surface intersects only the specified divertor surface, clearing the opposite divertor as well as the other internal components. The non-defining separatrix may coincide with the 2-cm surface but may not lie between it and the defining separatrix. The SN capability allows the plasma heat flux to be controllably deposited on either divertor target and can be used to correct for up-down imbalances caused by drifts or stray fields. It may also have the advantage of a lower H-mode threshold than that obtained in the DN mode when the ion  $\nabla B$  drift is toward the X-point.

In the IW mode, the last closed flux surface (LCFS) is tangent to the limiter and no sweeping is needed. The 2-cm surface intersects only the limiter, clearing both divertor targets, the outboard limiters, and the ICRF antenna. The separatrices may coincide with the 2-cm surface but may not lie between it and the LCFS. The IW mode provides the flexibility to operate in a non-divertor configuration. It also allows for energy sharing between the divertor and limiter in a hybrid operating scenario, thereby extending the burn time, provided H-mode confinement and acceptable impurity lev-

els can be sustained in the limiter phase of the discharge.

In keeping with the BPX mission, the first-wall (divertor and limiter) systems must absorb the thermal energy losses associated with up to 500 MW of fusion power. Accordingly, they are required to handle plasma losses of up to 100 MW for a heat load flattop of 3 s in addition to the heat load rise and fall times of about 5 s and 3 s, respectively. These requirements apply in the pure DN and IW operating modes. (A design study aimed at increasing the flattop time to  $>5$  s and providing greater margin against uncertainty is described in the appendix to this chapter.) The SN mode affords operational flexibility, as discussed previously, but does not drive energy handling requirements. Outboard limiters, both toroidal and poloidal, are also required for startup and for protection of the ICRF antennas and any other components (e.g., diagnostics) that may be mounted in the port region.

The energy handling capability is a function of the material properties and geometry of the first-wall components, of the (time-varying) magnetic field geometry in the periphery, of the transport of particles and energy in the scrape-off channel, of the partitioning among various energy loss mechanisms, and of spatial asymmetries in the energy flow. The BPX first-wall systems utilize thick tiles made of carbon-based materials with excellent thermal properties to rapidly conduct heat away from the surface and store it in the bulk. This design satisfies the requirements subject to a "standard" physics model that may be summarized as follows:

1. maximum temperature of first-wall surfaces 1700°C
2. pre-shot temperature of first-wall components at least 350°C
3. energy scrape-off distance 4 mm (DN) and 6 mm (IW), evaluated at the outboard midplane
4. conducted energy loss of 60% to the divertor plate (DN), 80% to the limiter (IW); remaining losses to radiation.
5. up-down energy flow asymmetry 1.2:1 (DN)
6. out-in asymmetry range from 4:1 to 2:1 (DN)
7. toroidal peak-to-average asymmetry 1.5:1.

The calculated divertor performance is illustrated in Fig. 2.5, in terms of the temperature history at three points on the outboard divertor surface for the DN operating mode with 500 MW of fusion power. In this calculation, the spatial asymmetries have been combined to reinforce each other, yielding a worst-case peak heat flux of  $\sim 50$

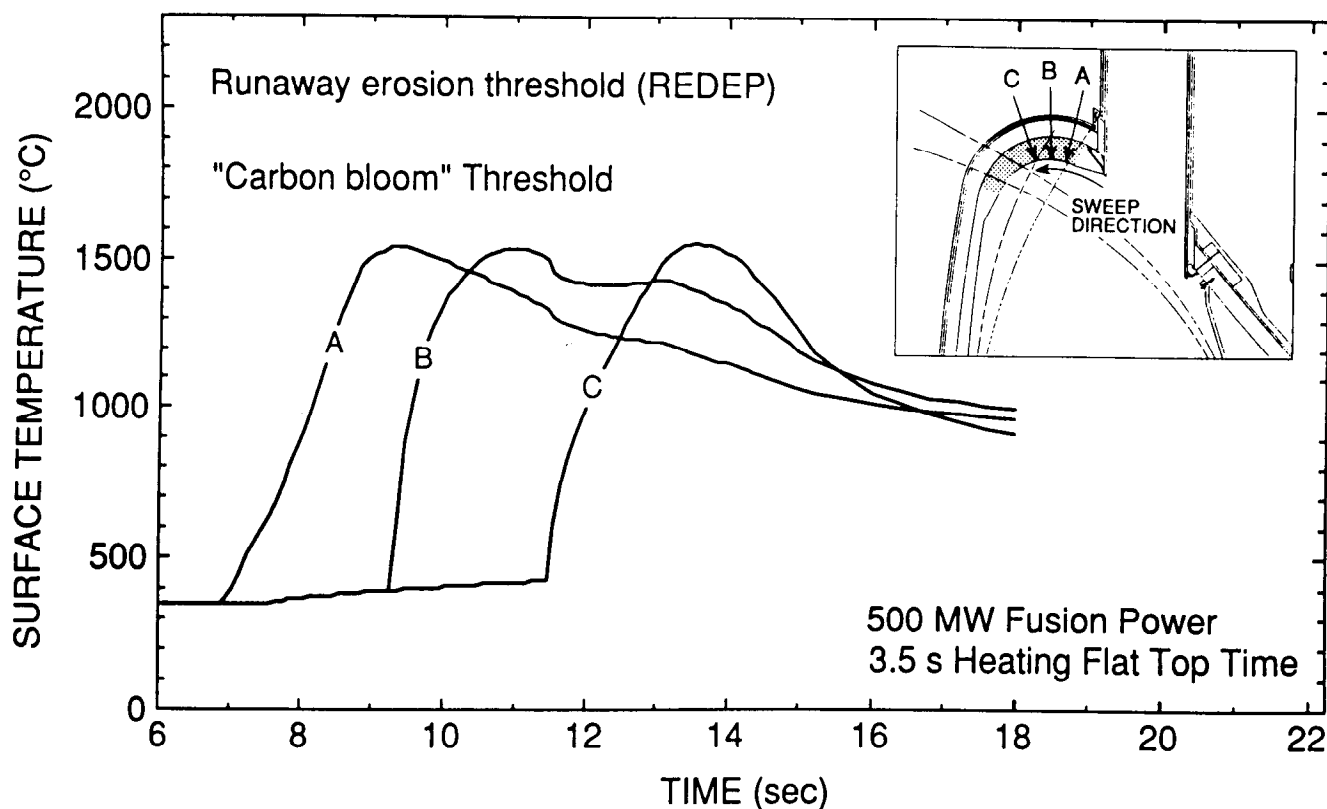


Fig. 2.5. Divertor surface temperature versus time at three points for reference DN divertor discharge with  $P_{fus} = 500$  MW. Temperatures remain below estimated thresholds for carbon blooms ( $1700^{\circ}\text{C}$ ) and runaway erosion ( $2000^{\circ}\text{C}$ ).

$\text{MW}/\text{m}^2$ . Nevertheless, the temperatures remain below the  $1700^{\circ}\text{C}$  temperature limit, as required. The basis for the physics model used here are described in more detail in Chaps. IX (geometry and energy flow issues) and X (impurity and materials issues).

Improvements in energy handling capability are clearly desirable in order to extend the flattop burn time beyond 3 s at the high-end fusion performance level. One way may be to reduce the peak divertor heat flux by enhancing the radiative losses; a gas puff system will be provided in the divertor region for this purpose. Another approach may be to utilize the combined capacity of the divertors and limiters by evolving from a DN to an IW mode in a single discharge. Higher first-wall temperature limits may be permissible with the high divertor densities expected in BPX. Careful position control or alternating SN operation may help to improve on the assumed up-down asymmetry. Similarly, careful component alignment and control of static field perturbations may result in improved toroidal symmetry. The flexibility to test these techniques is reflected in the design requirements because of

the importance of being able to optimize the energy handling capability. However, they are not included in our physics model because of the difficulty of quantifying their potential benefits.

Besides the thermal energy, the facility design must accommodate the radiated energy (in neutrons and gamma rays) associated with burning plasma operation. It is required to be compatible with peak radiation fluxes corresponding to  $P_{fus} = 1000$  MW. It must also be compatible with integrated fusion yields of up to 4 GJ ( $1.5 \times 10^{21}$  neutrons) per pulse, up to 2.5 TJ per year, and up to 6.5 TJ over the facility's lifetime. These requirements affect the design of vacuum vessel, coils, ICRF antennas, and several diagnostics, all of which are shielded from the reacting plasma only by the structure itself. They also affect the test cell, which is the primary radiological shield for personnel. One consequence of the requirements is that no personnel access to the test cell will be possible (except in the initial hydrogen operation), making remote maintenance a necessity.

In summary, BPX discharges are designed to maximize the pulse length and burn time available

within the constraints of inertially cooled magnets and first-wall components and limited shielding. A set of reference operating modes defines the minimum configuration and energy handling requirements. Additional capabilities are specified to provide the flexibility needed to optimize energy handling capability.

#### II.D. PLASMA MAGNETICS AND DISRUPTION HANDLING

The required operating modes for BPX demand an exceptional degree of control over the magnetic configuration. Divertor sweeping with minimum X-point-to-target spacings ( $\geq 15$  and  $\geq 10$  cm), scrape-off channel width ( $\geq 2$  cm), and ICRF antenna conformity ( $\pm 1$  cm) are all prescribed. Thus, in a machine with a 12-m overall diameter, the interface between the plasma boundary and internal components must be controlled with tolerances of order 1 cm. The discharge time evolution must be programmed in such a way as to make optimum use of the available flat-top time and energy handling capacity. These considerations affect the design of the PF system, which consists of seven up-down coil pairs external to the TF coils and two pairs internal to the TF coils (Fig. 2.1). The external coils (three solenoid and four "ring" coil pairs) provide the volt-seconds (77) for inductive current drive and the equilibrium fields for shape control. Three of the seven pairs are driven asymmetrically to accommodate the SN operating mode. The internal control (IC) coils provide the fast response capability required to control the vertical instability and react to minor disruptions.

Most of the control requirements, e.g., the required flux swing or equilibrium field characteristics, are implicit in the specifications for the required reference operating modes, so the GRD need not explicitly define them. Additional radial and vertical position control requirements that are defined in the GRD are

1. to provide radial control such that an instantaneous change in  $\beta_p$  of  $-0.2$  results in a position change of the inboard boundary of a diverted plasma of less than 3 cm. This is required to accommodate plasma equilibrium perturbations, including minor disruptions, that can cause rapid shifts in radial position.
2. to provide radial control such that the position of the outboard plasma boundary can be maintained within  $\pm 1$  cm of any location within a 4-cm range. This is required to control ICRF antenna loading.
3. to provide vertical control capable of stabilizing the vertical instability and accommodating a 2-cm variation in plasma position. The

system must be able to compensate for stray radial fields characterized either by rapid random fluctuations or by quasi-dc secular drifts.

All the control requirements are satisfied subject to physics models for magnetohydrodynamic (MHD) equilibrium and stability, magnetic diffusion, breakdown, and volt-second consumption. These models and related analyses are described in detail in Chap. V.

Limits on TF ripple are chosen to reduce classical fast alpha-particle losses to negligible levels. Within  $R < R_0 + a/2$ , the peak-to-average ripple must be  $\leq 0.3\%$  over the plasma cross section, and even lower,  $\leq 0.1\%$ , on the midplane. Details of the models and analysis are provided in Chaps. III and V.

Limits on nonaxisymmetric error fields are set to avoid the adverse effects attributed to resonant helical field perturbations. Examples are heat load redistribution and disruptivity enhancement due to mode locking. Much of the experimental data on this topic has been supplied by DIII-D, and our requirement is an adaptation of criteria that they have developed.

The Fourier harmonic amplitudes  $(\delta B_r)_{m,n}$  of the magnetic error field on a circular-cross-section torus of major radius  $R_0$  and minor radius  $a$  must satisfy the inequality

$$\sum_{1 \leq m/n \leq 5} \frac{1}{n} \sqrt{\frac{m(\delta B_r)_{m,n}}{B_T}} < 0.05.$$

This applies to harmonics with toroidal mode number  $n = 1$  to 6. The requirement extends to  $n = 6$  perturbations because of the segmentation of the TF and IC coil systems into six modules.

This requirement implies tight tolerances on the toroidal symmetry of the coil systems and on the placement of coil feeds and buswork. For example, the concentricity requirement on the high-current-carrying PF coils is a few millimeters. A simple, unoptimized field perturbation coil has been effective in controlling operational limits in DIII-D (Ref. 2). In BPX, active field perturbation control will be provided by a system of three "window frame" coils located in the vicinity of the outer ring coils in each hexant. The design is based on that of an optimized coil set planned for DIII-D. It can be used to compensate for field errors due to PF and TF coil displacements. It may also allow controlled field perturbations to be *imposed* to produce ergodic field lines in the divertor region as a means of moving hot spots around the machine to avoid overheating of isolated areas. Field error requirements, models, and analyses for BPX are described in more detail in Chap. V.

Although the BPX operating regime lies well within normal stability boundaries, the possibility of major disruptions cannot be realistically excluded. Because of the high magnetic and thermal energies stored in the plasma, the loads imparted to the vacuum vessel, internal components, and PF coils when the plasma disrupts are potentially quite severe. Due to its effect on the radial build of the tokamak, the most crucial region is near the inboard vessel wall, particularly the joint between vessel segments, and the inner limiter tile supports. To accommodate the expected loads on the vessel, a high-strength alloy (Inconel 625) is used, with a wall thickness of 7 cm and a joint thickness of 11 cm. Clearly, the requirement to withstand disruptions drives the structural design of several systems and has a major overall impact on the device.

The disruption handling requirements for BPX are derived from the world tokamak data base and a calibrated model incorporated in TSC. The model includes both radial and vertical plasma drifts and both toroidal and poloidal eddy currents. Also included are "halo" currents that flow along open field lines in the plasma scrape-off layer and through a return path provided by the first-wall tiles and vacuum vessel. These currents, which impact the time evolution of the disruption and the spatial distribution of forces, have been observed on DIII-D, JET, and PBX-M, where they have resulted in substantial component displacements. The BPX design must accommodate major disruptions with a frequency of 10% in any mode of operation, characterized by

1. thermal quench in 0.1 to 1.0 ms
2. current quench rate up to 3 MA/ms
3. poloidal halo currents up to 2 MA
4. either mainly vertical or mainly radial plasma motion.

A range of disruption events is modeled to ensure that worst-case loads are revealed. The most severe are the vertical displacement events (VDEs), in which the plasma drifts several tens of centimeters vertically, until  $q_{95} \approx 2$ , before disrupting. The severity of these events appears to be connected with the accompanying halo currents and strong up-down asymmetry in the loads (Fig. 2.6). Further details of the disruption models, analyses, and physics basis are provided in Chap. V.

## II.E. HEATING, FUELING, AND WALL CONDITIONING

Auxiliary heating systems are required to heat the plasma to reaction temperatures and to maintain power balance under subignited conditions. The baseline heating method is ICRF, with 20 MW

coupled to the plasma, as discussed in Sec. II.B. Four of the twelve large radial ports are allocated for the ICRF antennas needed to supply this power. The GRD also requires that the device and facility be able to accommodate future heating upgrades: either an additional 10 MW of ICRF (30 MW total) or 30 MW of ECH (50 MW total). The additional power afforded by these upgrades would provide greater flexibility for driven operation and a wider operating space. The ECH option offers the potential advantages of localized heat deposition and control of instabilities.

The ICRF system is required to operate for 15-s pulses in order to heat during the rampup and rampdown as well as the flattop. The standard heating mode utilizes  $^3\text{He}$  minority with a deuterium or D-T majority. In the latter case, minority heating is superseded by tritium second-harmonic heating as the temperature rises. The system must therefore supply full power in frequency bands in the range of 60 to 90 MHz to be compatible with toroidal fields from 6 to 9 T. The output power must be feedback controllable in order to regulate the fusion power output. Further details of the heating systems and the corresponding physics analyses are given in Chaps. VI (ICRF) and VII (ECH).

Plasma fueling systems are required to supply the initial fill gas to form the plasma and later to raise the density and balance particle losses. In BPX, both gas and pellet injection systems are required for flexibility. Gas injection is implemented in both the midplane (for initial fill and edge density control) and in the divertor region (for divertor heat load reduction). However, because of the low fueling efficiency of gas puffing and the need to maintain a low in-vessel tritium inventory, tritium fueling will be accomplished by pellet injection. The pellet injection system includes both 1.5 km/s and 4 to 5 km/s guns for density profile control. The maximum particle source rate for the pellet systems is about  $10^{22} \text{ s}^{-1}$ , driven mainly by makeup fuel requirements under minimum-recycling conditions. Fuel particles will be exhausted passively by surface codeposition in the moderate-temperature regions of the carbon tiles. Further details on the fueling systems and physics are given in Chap. VIII, and details on particle exhaust are given in Chap. X.

Wall conditioning is an important element in the particle control strategy (for both fuel and impurities) in BPX. The vessel and all internal components will be baked to 350°C to drive out trapped impurities. Glow and pulsed discharge cleaning systems, with the walls at 350°C, are also required. Discharge cleaning gases will include  $\text{H}_2$ ,  $\text{D}_2$ , helium, and  $\text{He-O}_2$  mixtures; the last is required to

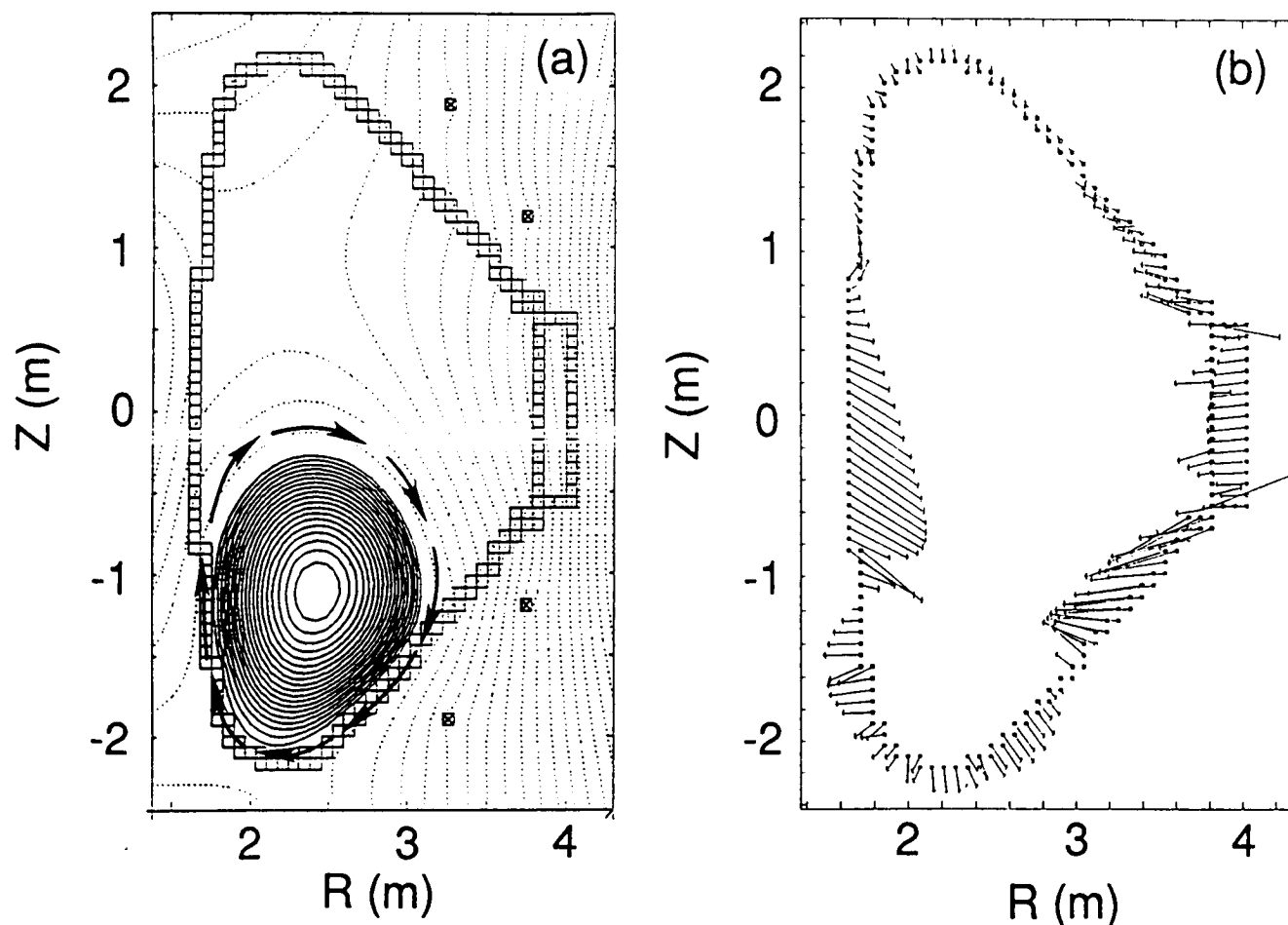


Fig. 2.6. Snapshot during current quench phase of a VDE disruption, as calculated by TSC. Bold arrows in left frame represent poloidal "halo" current flow. Arrows in right frame represent magnitude and direction of electromagnetic forces.

remove tritium codeposited with carbon, for inventory control purposes. Helium may also be effective for removing recently deposited tritium between shots. The first-wall components are also required to operate at a pre-shot temperature of  $350^{\circ}\text{C}$ . The capability for boron deposition by glow discharge will be provided. The wall conditioning requirements are motivated by considerations of impurity control (particularly oxygen), fuel recycling control, tritium inventory control, and recovery from disruptions. Further details are presented in Chap. X.

## II.F. DIAGNOSTICS

A set of physics diagnostics is required to fulfill the BPX mission objectives. A range of alpha-related measurements is clearly needed, in view of BPX's programmatic focus on the physics of burn-

ing plasmas. To fully characterize such plasmas also requires that the main plasma parameters be accurately determined as functions of space and time. The main design issues for diagnostics are those associated with the space limitations in the device and facility, the harsh operating environment, and remote maintainability. Development is needed to produce the new diagnostics required for alpha-particle measurements and to adapt more traditional diagnostics to the BPX application. An overview of the diagnostic requirements and a summary of planned diagnostics are given in Chap. XI. The measurement requirements are as follows:

1. **Plasma control:** magnetic diagnostics for plasma and vessel currents, plasma position and shape, and locked-mode indication; line-averaged density for control purposes; divertor and limiter surface temperatures

2. **Confinement:** core profiles of electron density and temperature, ion temperature, average impurity concentration, and radiated power; poloidal beta; low- $Z$  and high- $Z$  impurity concentrations; relative deuterium, tritium, and helium ion concentrations
3. **Fluctuations and wave activity:** internal and external fluctuations over a frequency range adequate to encompass MHD activity, internal turbulence, and projected alpha-driven instabilities
4. **Divertor and edge plasma:** electron density, ion and electron temperatures, bulk ion and impurity behavior
5. **Fusion yield:** total neutron flux, neutron fluence, neutron source radial profile; fast-confined and slowed-down alpha density and energy distribution; escaping alpha flux and velocity distribution.

Some of these measurements are required for operational as well as research purposes, such as those of plasma current, position, and shape; divertor and limiter surface temperatures; deuteron:triton density ratio; and fusion power.

## II.G. OPERATION

Operating lifetime and schedule considerations have an important influence on the design of the machine. Clearly, enough shots must be provided to accomplish the mission objectives, and at an adequate repetition rate to permit efficient optimization. From an engineering standpoint, the number of shots determines the fatigue-life criteria for structural components, but does not represent a sharp limit. The total radiation fluence, which impacts the design of insulators and diagnostic components, also depends on the number of fusion plasma shots. The repetition rate requirements determine the design of cooling systems for the coils, vacuum vessel, and first wall; tritium inventory control procedures; and maintenance schedules. Although it is likely that many more than the required minimum numbers of pulses listed below will be attainable, the operation plan (Chap. XII) has been developed so as to accomplish the mission within these numbers. The operational requirements specified in the GRD are as follows:

1. Minimum number of pulses:
  - (a) 3000 at  $B_T = 9$  T and  $I_p = 11.8$  MA (for burning plasma studies requiring maximum performance)
  - (b) 30 000 at  $B_T = 6$  T and  $I_p = 7.9$  MA (for optimization and low- $Q$  physics studies; also essential for ICRF commissioning

since the standard heating mode can be replicated at 60 MHz).

- (c)  $6 \times 10^6$  for pulsed discharge cleaning
2. Minimum repetition rates in reference operating modes:
  - (a) 1 pulse per hour
  - (b) 16 pulses in 16 hours in consecutive 8-hour shifts
  - (c) 1000 pulses per year
3. Maximum scheduled maintenance downtime:
  - (a) maximum of 4 months per year, averaged over the life of the device following initial D-T shakedown

The GRD also specifies requirements on reliability, availability, and maintainability (RAM). These primarily affect the engineering design of individual subsystems. However, since the motivation for the RAM requirements is to ensure a sufficient level of availability and reliability to carry out the physics mission, we briefly summarize them here:

1. **Operational availability:** 80%. Defined as the ratio of the number of shots in which the device is operational at rated performance to the number of potential rated performance shots in the absence of failures.
2. **Shot reliability:** 90%. Defined as the probability that, once initiated, a shot's objectives will be achieved; i.e., all components function properly, all necessary data are logged, and no failure occurs that would preclude the next shot.
3. **Mission reliability:** The facility must provide for recovery from all failures having a probability of occurrence greater than  $10^{-4}$  per year that would compromise the mission by precluding operation at full parameters.
4. **Maintainability:** The design must provide maintenance capability consistent with meeting the above availability and reliability requirements, the scheduled maintenance downtime requirements, and the radiological requirements. In effect, this means that extensive remote maintenance capability inside the test cell must be provided.

## II.H. TOKAMAK SYSTEM DESIGN

So far in this chapter, we have summarized the general physics requirements for BPX. We conclude by briefly describing some of the main engineering features of the tokamak device. Later chapters will provide further details on the heating, fueling, and energy handling systems.

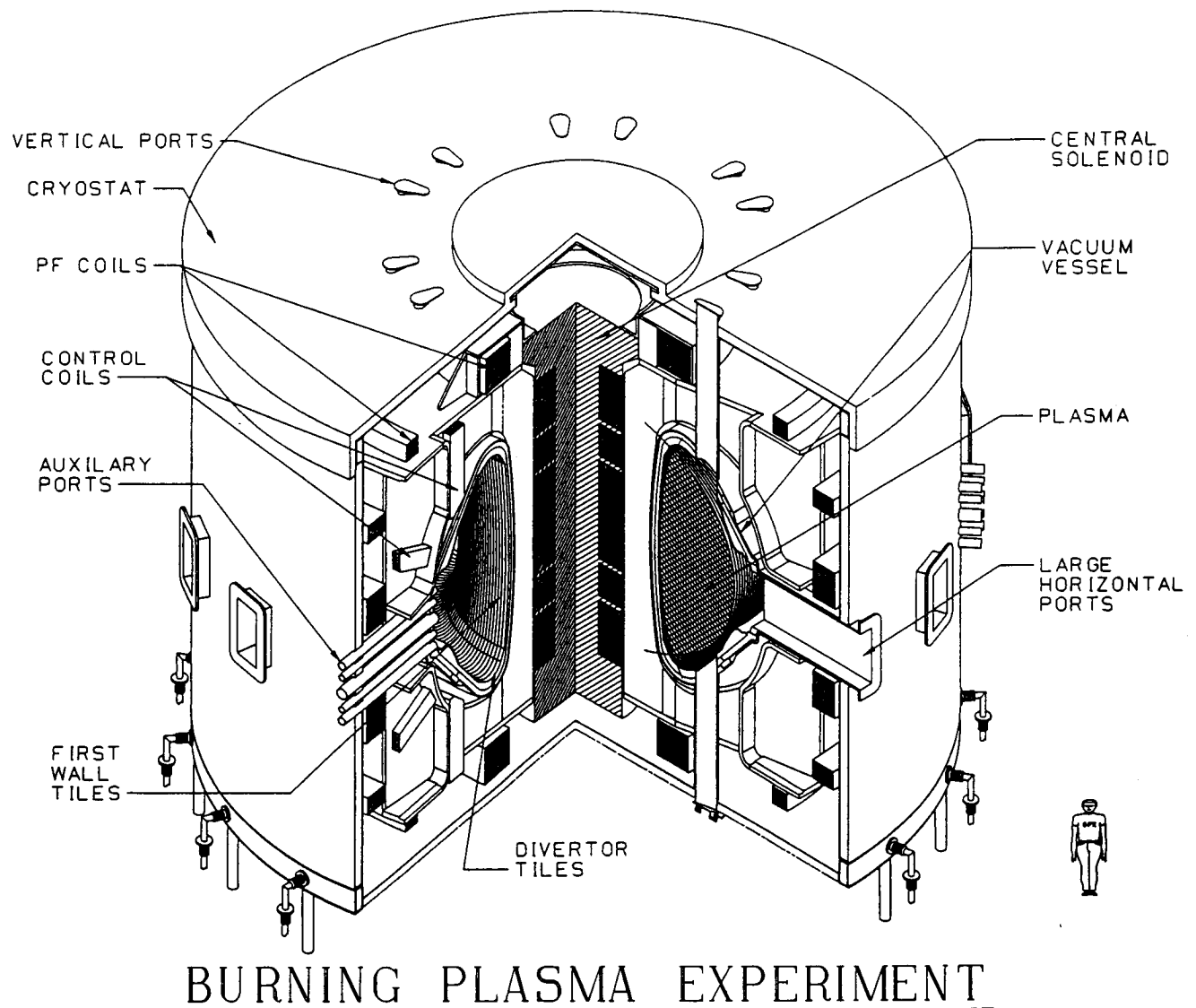


Fig. 2.7. Cutaway view of the BPX device.

A cutaway view of the BPX is shown in Fig. 2.7. To facilitate assembly, a modular design approach is used. There are six modules, each consisting of three TF coils, a vacuum vessel segment, and four IC coil segments. Each TF coil case is welded to its neighbors both within and between modules. The centering forces are reacted by wedging of the coil inner legs. The vessel segments are bolted together structurally, with a welded vacuum seal. The vessel is supported by six vertical legs extending from the underside of the vessel to the TF structure in the joint region. First-wall components are supported directly off the vacuum vessel. The central solenoid consists of three PF coil pairs assembled as a unit. The IC coil segments are electrically connected by module-to-module jumpers.

The TF system consists of 18 identical coils arranged three to a module in a wedged support configuration. The TF coil cases are constructed of thick plates of 316LN stainless steel, a high-strength structural alloy, welded together as shown in Fig. 2.8. Each case encloses all but the inner leg of the conductor assembly, which is wedged against the adjacent conductor. The conductor is of plate construction. Each coil has 21 turns, with each turn constructed from three plates welded together. The conductor material is beryllium copper, which offers high strength (110 ksi at a temperature of 293 K) but reduced electrical conductivity [57% Internationally Accepted Copper Standard (IACS)]. In operation, the coils are cooled to liquid nitrogen temperature using cooling lines

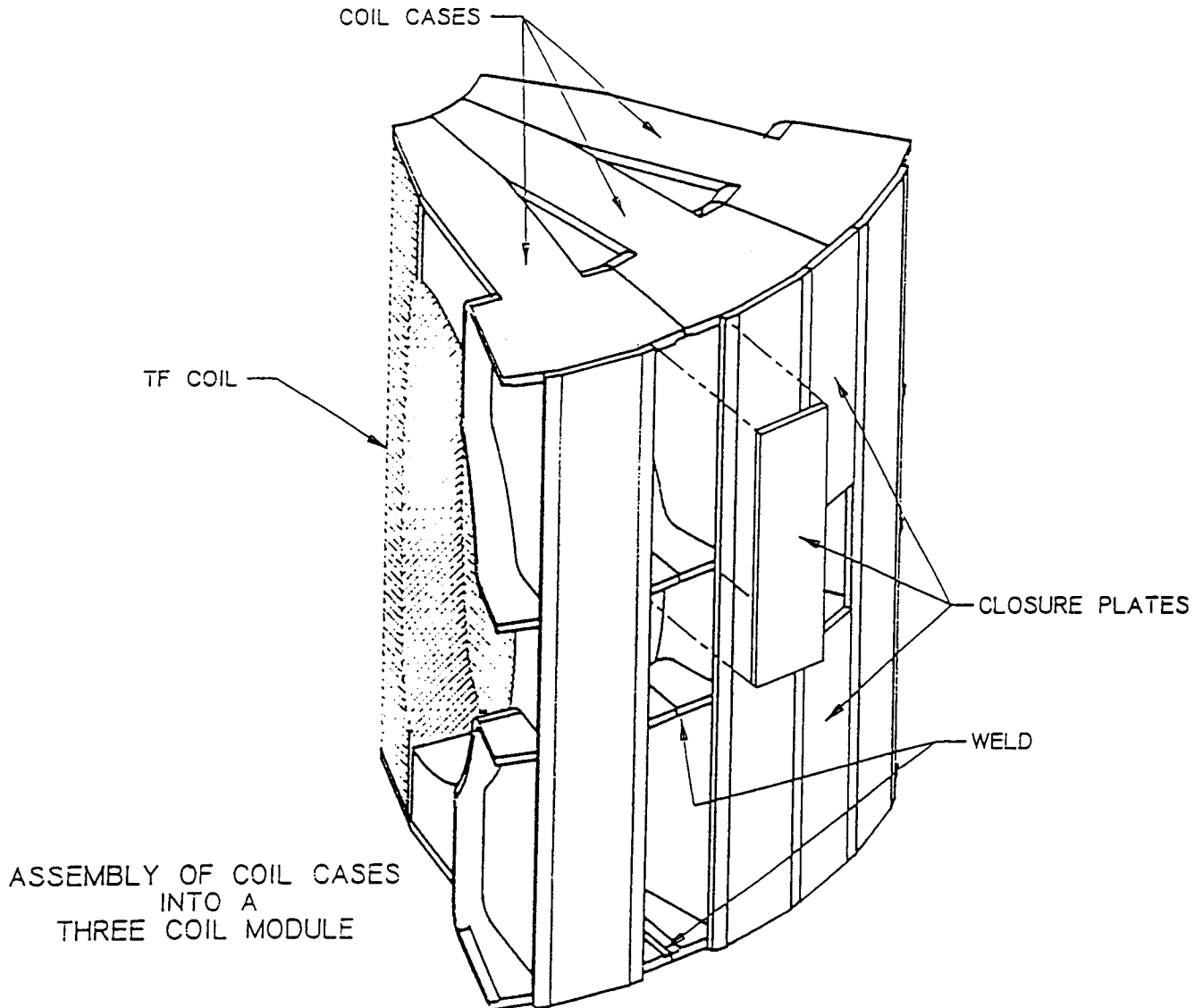


Fig. 2.8. Assembly of three TF coils into one of six modules. Coil cases and cover plates are made of thick stainless steel plates fastened together by welding.

welded to the edge of the plates. During a pulse, joule and nuclear heating of the coils raise them to about room temperature. The coils will draw up to 20.5 GJ of electrical energy (of which 13.0 GJ is dissipated resistively and 7.5 GJ is stored in the magnetic field), at a peak power of 650 MW. The electrical energy is supplied from flywheel motor-generator systems through a thyristor-controlled rectifier system.

The PF coil system includes seven up-down coil pairs external to the TF, as shown in Fig. 2.1 and described in Sec. II.D. The PF system provides 77 volt-seconds for inductive current drive, as well as the equilibrium fields for plasma shape control. Fast time scale radial and vertical position control are provided by the IC coils. Like the TF, the PF

coils are precooled to liquid nitrogen temperature before each pulse. Current waveforms for the reference DN operating mode are shown in Fig. 2.9. These are obtained through an optimization procedure in which the equilibrium and volt-second requirements are satisfied while minimizing peak stresses and electrical energy consumption. The maximum electrical energy used is about 5.2 GJ and peak power is about 600 MW.

The divertor and limiter systems utilize thick tiles made of carbon-based materials to absorb the plasma's thermal energy losses while maintaining a low  $Z_{eff}$ . The design concept for the divertor tile assemblies is shown in Fig. 2.10. Pyrolytic graphite is used for the divertor and a carbon-carbon fiber composite is used for the limiter; Inconel is used for

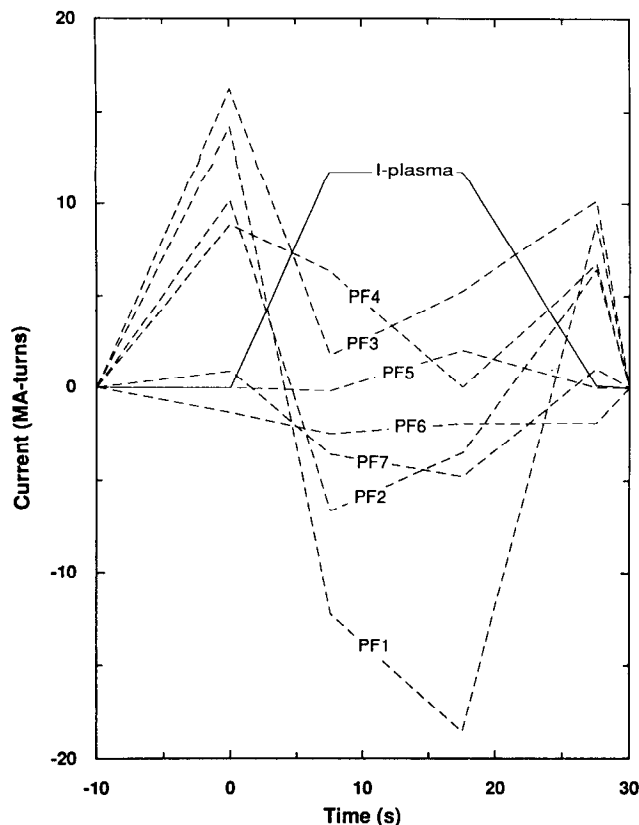


Fig. 2.9. Poloidal field coil and plasma current waveforms for the reference double-null divertor operating mode.

the structural components. Key design features include (a) compactness to minimize radial build; (b) small component size and high strength for disruption survival, and (c) remote maintainability. The tiles are operated at a minimum pre-shot temperature of  $350^{\circ}\text{C}$ . During a shot, the surface temperatures reach up to  $1700^{\circ}\text{C}$  in regions of high heat flux. Heat is stored in the tile bulk during the pulse and transferred to the vacuum vessel by radiation and conduction between pulses.

The vacuum vessel serves several purposes. It maintains base vacuum conditions with partial pressures  $<1 \times 10^{-7}$  Torr for hydrogen and  $<1 \times 10^{-9}$  Torr for impurities, serves as the heating and cooling path for the first wall, provides mechanical support for internal components and diagnostics, and provides passive stabilization for the vertical instability. The vessel is constructed of thick, high-strength materials (Inconel 600 and 625) to be able to withstand the electromagnetic forces imposed by disruptions. Each of the six vessel segments is fitted with two large ( $0.46 \times 1.02$  m) radial ports (for a total of 12), four vertical ports, and six smaller diameter (10 and 18 cm) radial ports adjacent to the joints.

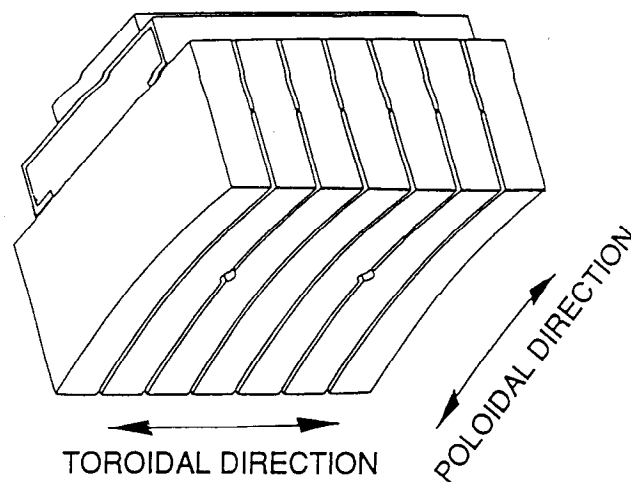


Fig. 2.10. Divertor tile assembly.

### III. SUMMARY

A set of requirements and a conceptual design for BPX have been developed that meet the BPX mission objectives. The tokamak and the heating and fueling systems will provide the plasma performance necessary to reach the burning plasma regime. Energy and particle handling by the divertor and inner-wall limiter will permit burn times of several energy confinement times at full performance and much longer pulses at minimum performance. Because of uncertainties in the physics models used to project energy handling, however, flexibility is incorporated to optimize this aspect of the device's performance during the operating phase. Discharge scenarios have been developed to provide a basis for the design of the magnetic, heating, fueling, and energy handling systems, and detailed disruption scenarios have driven the structural design of the vacuum vessel and other device components. The diagnostic requirements focus on plasma control, confinement, fluctuations, waves, and fusion yield. Operational planning is driven by considerations of fatigue life, shot repetition rate, and the access limitations that will be imposed by burning plasma operation. High reliability and maintainability are required to ensure a level of availability sufficient to complete the BPX mission.

The BPX physics and engineering studies have led to the definition of a tokamak facility that will provide a unique opportunity to explore a new physics regime in which alpha-particle heating is dominant. In the remainder of this paper we describe the physics basis for the requirements that

have been set and the physics-based analysis that helps support the chosen design.

#### APPENDIX: DIVERTOR OPTIMIZATION

In the baseline BPX design upon which this paper is based, the burn pulse at  $P_{loss}=100$  MW is limited to a 3-s flattop, with a 5-s heating and a 3-s cooling phase. However, the 10-s magnet flattop time and the desirability of increasing the margin against divertor performance uncertainties are incentives to further optimization of the divertor design. In this appendix, we describe improvements to the divertor geometry that resulted from a very recent study that successfully addressed these two objectives.

The divertor performance projections depend on material properties, operating temperatures, edge plasma conditions, partitioning among the various loss channels, heat flux uniformity, and divertor geometry. Each of these factors has uncertainties associated with it that could limit performance at  $P_{fus} = 500$  MW (although the margin at the minimum level,  $P_{fus} = 100$  MW, is ample). Thermal shock resistance considerations could force the use of a material with 10 to 20% lower thermal performance.<sup>3</sup> Improved erosion estimates and impurity control considerations could change the temperature limit by  $\sim 200^\circ\text{C}$  in either direction. Uncertainties in edge density and transport coefficients translate into an estimated uncertainty factor of  $\sim 1.4$  in peak divertor heat flux.<sup>4</sup> Strict impurity control measures are planned (e.g., operation with hot walls and boronization) that may keep the radiated loss fraction less than the assumed 40%, thereby increasing the heat flux to the divertor. Field errors could increase toroidal heat flux peaking factors above the assumed 1.5:1, and  $E \times B$  drifts or imperfect vertical position control could raise the up/down heat load imbalance above the assumed 1.2:1. Small deviations from the optimum sweep trajectory, due to uncertainties in either the magnetic measurements or control, could result in divertor heating patterns that exceed temperature limits in some regions. Many techniques have been suggested to improve divertor performance such as gas targets, impurity seeding, ergodization, and toroidal sweeping. All of these will be tested in BPX. However, the most straightforward and readily quantifiable optimization approach is to improve the geometry.

Any optimization must be constrained by physics requirements and by the geometry of neighboring components. The plasma elongation  $\kappa_{95}$  is limited by the ability to control the vertical instability. The range of triangularity  $\delta_{95}$  is determined by the divertor sweep limits, though the results of the optimization turn out to be favorable for

MHD stability. For global stability, the safety factor at the 95% flux surface  $q_{95}$  is required to remain  $\geq 3.2$  throughout the pulse. For power handling purposes, the optimum sweep trajectory is obtained with constant  $q_{95} \equiv 3.2$ , since this maximizes the sweep length while exceeding the minimum X-point to target distances (15 cm for the outer and 10 cm for the inner divertor leg). This results in  $\kappa_{95}$  decreasing during the sweep from 2.08 to 1.91 as  $\delta_{95}$  increases from 0.23 to 0.42. The X-point thus follows a nearly linear trajectory sloping inward and toward the horizontal midplane, as shown in Fig. 2.11.

In modifying the physical geometry, the inboard end of the divertor target was constrained by the TF coil. High stresses in that region of the coil preclude any reduction in its cross section that would permit displacement of the divertor away from the plasma. The outboard end of the divertor target, however, was shifted vertically outward to increase the swept area by tilting the target with respect to the incident field lines. The amount of displacement was constrained by TF coil fabrication considerations and the need to limit the increase in machine size and cost. The resulting growth in the overall TF coil height was only 14 cm, or 2.2%. The resulting divertor profile is a nearly flat surface parallel to the X-point trajectory. This is shown in Fig. 2.11, where the comparison with the previous divertor can also be seen.

The outer sweep limit is constrained by the position of the vertical port. To avoid high heat fluxes on the port's toroidally facing sidewalls, the sweep must start at least 8 cm from the inner edge of the port. The inner sweep limit is constrained by the requirement that the outer separatrix may not oversweep any area swept by the inner separatrix. This segregation permits the use of a "sawtooth" arrangement, as discussed in Chap. X, to protect leading edges of tiles from extreme heat fluxes. A tile can be tilted to match either the inner or outer divertor field line angle, but not both. The sweep limits were chosen, subject to these constraints, to provide the maximum sweep distance. The new distance is  $\sim 40$  cm, as compared to 20 cm in the baseline design. This is a substantial increase that produces a corresponding increase in performance.

To evaluate the performance, we combine a physics simulation of the discharge evolution with an engineering analysis of the material's thermal response. A sequence of equilibria satisfying precise shape constraints, calculated with the control matrix equilibrium code BEQ, is used to map the time-varying magnetic geometry in the divertor region. The time behavior of global equilibrium parameters (such as  $\beta_p$  and  $l_i$ ) and plasma energy losses is based on the reference 500-MW discharge

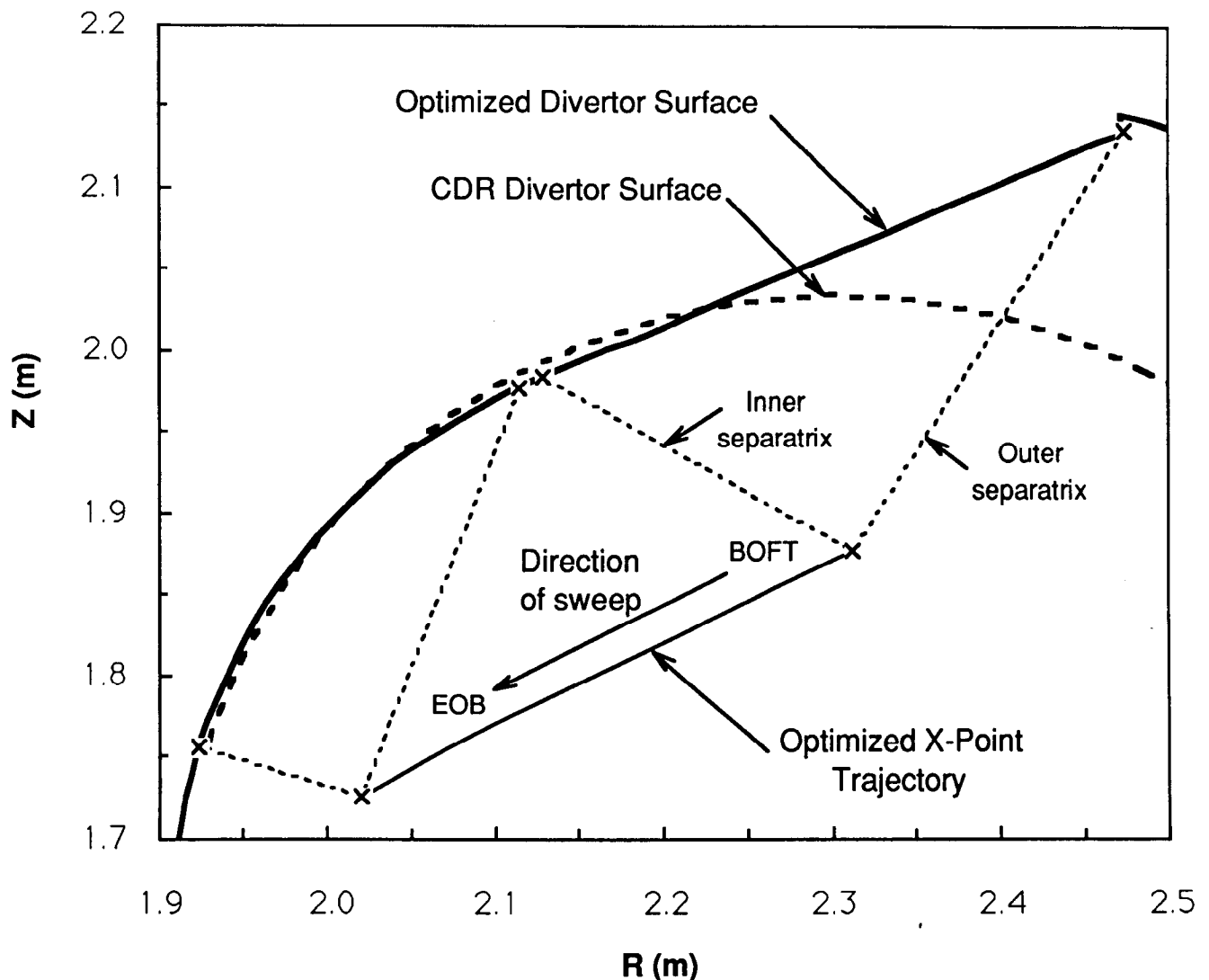


Fig. 2.11. Optimized BPX divertor geometry showing the X-point trajectory, divertor separatrices at the beginning of flattop (BOFT) and end of burn (EOB), and divertor profile. CDR divertor profile shown dashed.

simulations calculated with the TSC code and described in Chap. V. The energy losses are partitioned among the various loss channels and among the four divertor channels (up/down, in/out) according to the standard BPX guidelines. With 100 MW of total loss, a maximum of 26 MW flows to an outer divertor channel (upper or lower) under these guidelines. The heat flux is assumed to have an exponential profile at the midplane, with a scrape-off width  $\lambda_q$  of 4 mm, and to flow along field lines to the divertor. Here we use an equivalent  $\lambda_q$  derived conservatively from B2 code modeling of the scrape-off plasma.<sup>4</sup> During the sweep, the angle between the flux surface and the target varies from 34 to 45 degrees, the distance from X-point to target varies from 31 to 27 cm, and the flux

surface spreading factor relative to the midplane varies from 6 to 10. The peak heat flux parallel to the flux surfaces at the divertor target is about 60 MW/m<sup>2</sup>, but the surface heat flux is only 40 MW/m<sup>2</sup> due to the tilting of the target. The peak parallel heat flux is higher than that reported in Ref. 4 and in Chap. IX, both of which are based on the baseline design, because of (a) the inclusion of an assumed 1.5:1 toroidal peaking factor, (2) a reduction in the flux surface spreading at the target due to the longer X-point to target distance of the new geometry, and (c) the use of a conservative model profile that is narrower than those obtained from B2 with standard assumptions. The divertor temperature response is calculated using a one-dimensional transient thermal model, includ-

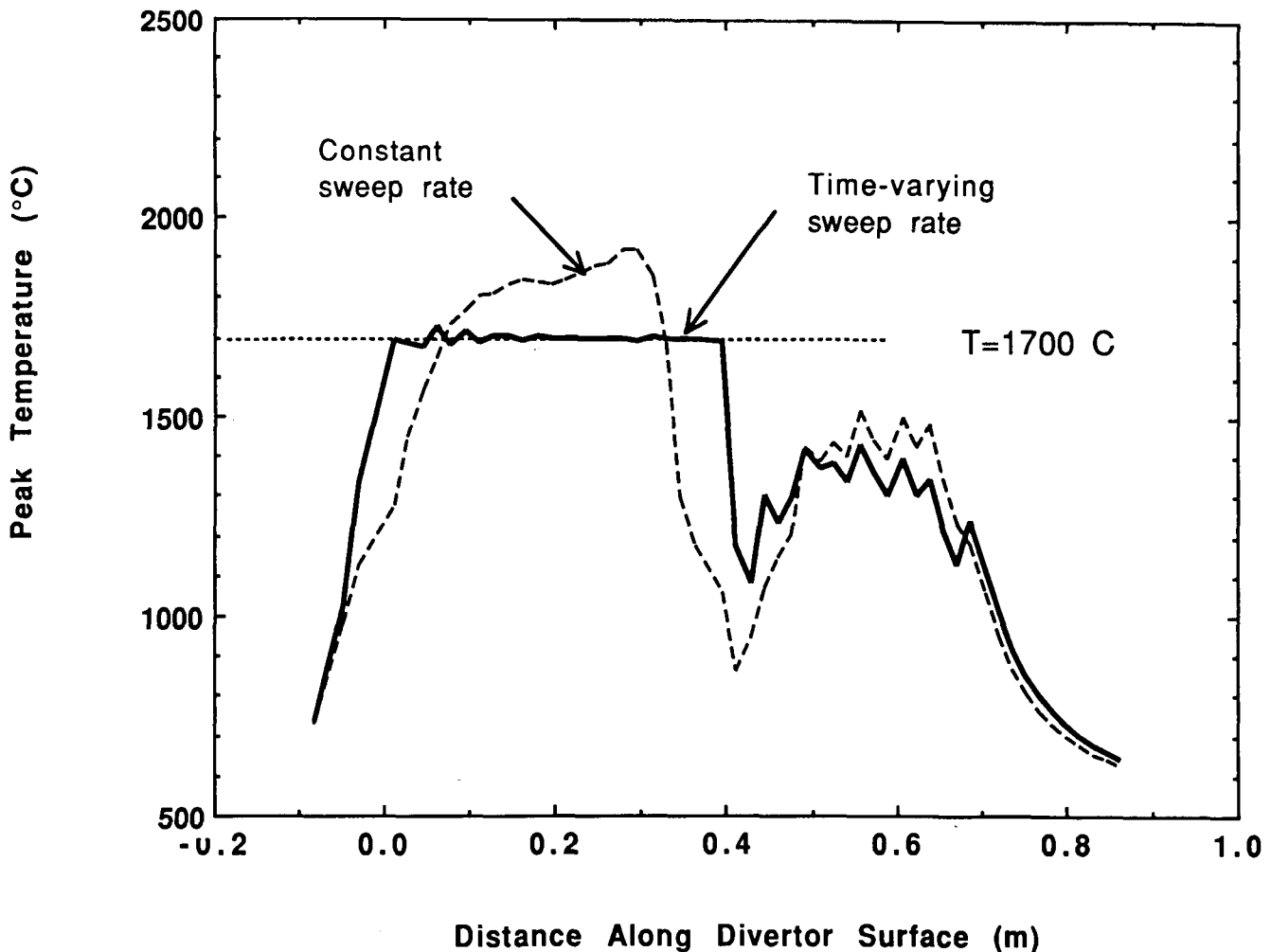


Fig. 2.12. Peak-temperature distribution along divertor surface with constant-velocity sweep and optimized sweep.

ing the temperature-dependent material properties. The analysis covers a sequence of several full-power discharges at one-hour intervals, to account for thermal ratcheting, with an initial temperature of 350°C.

As a first iteration, the divertor is assumed to be swept with a constant outer strike-point velocity. With this assumption, the flattop burn time (defined as the interval in which  $P_{loss}$  exceeds 95 MW) is limited by the 1700°C temperature limit to 3.7 s. However, most of the surface remains much cooler, representing unused heat capacity. The performance is improved by allowing the sweep velocity to vary as a function of time. The optimum sweep is that which results in 1700°C peak temperatures everywhere on the outer divertor surface, as depicted by the solid curve in Fig. 2.12. The flattop burn time for this idealized case is 7 s. A constant-velocity sweep of the same duration would cause the divertor to overheat, resulting in a large impu-

rity influx and premature discharge termination.

By optimizing the divertor geometry, the nominal flattop burn time for the case with 100 MW of loss has been increased from 3 to 7 s, both projections based on a velocity-optimized sweep. Allowing some margin for less than ideal plasma control and other uncertainties, we believe that a 5-s flattop is a realistic projection. Besides improved performance and increased margin, the modified geometry provides additional volume between the plasma and the vacuum vessel near the divertor, as can be seen in Fig. 2.13. This affords the possibility of incorporating advanced divertor concepts as a future upgrade to enhance particle control capabilities. The displacement of the outer walls of the vacuum vessel away from the plasma to accommodate the larger divertor has a potentially negative impact on vertical position control. However, a pair of simple passive toroidal conductors made of the vacuum vessel material will be added, as shown

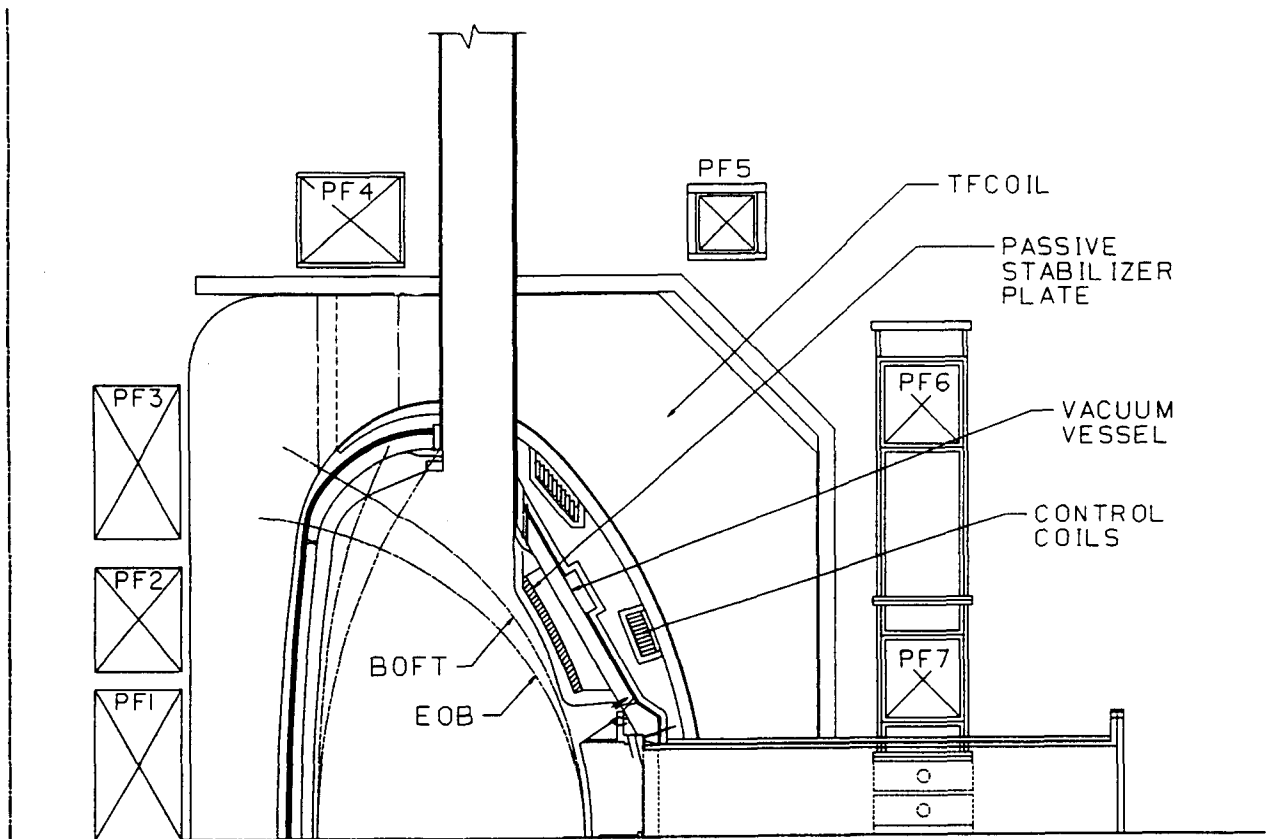


Fig. 2.13. Elevation view of BPX showing optimized divertor geometry and passive stabilizer plates.

in Fig. 2.13, to offset this.

#### REFERENCES

1. D. E. POST et al., "ITER Physics," ITER Documentation Series No. 21, International Atomic Energy Agency (1991).
2. J. T. SCOVILLE et al., *Nucl. Fusion*, **31**, 875 (1991).
3. J. R. HAINES et al., "BPX Divertor Design and R&D Program," *Proc. 14th IEEE/NPSS Symp. Fusion Engineering*, San Diego, 30 Sept.-3 Oct., 1991, to be published; and M. D. McSMITH et al., "BPX Divertor Conceptual Design and Analysis," *Proc. 14th IEEE/NPSS Symp. Fusion Engineering*, San Diego, 30 Sept.-3 Oct., 1991, to be published.
4. D. N. HILL et al., "Operating Conditions of the BPX Divertor," *Proc. 18th Eur. Conf. Controlled Fusion and Plasma Physics*, Berlin, 3-7 June 1991, Vol. III, p. 233.
5. D. J. STRICKLER, G. H. NEILSON, S. C. JARDIN and N. POMPHREY, "Plasma Shape Control Calculations for BPX Divertor Design," *Proc. 14th IEEE/NPSS Symp. Fusion Engineering*, San Diego, 30 Sept.-3 Oct., 1991, to be published.